# Vibrational assignments and line shapes in inelastic tunneling spectroscopy: H on Cu(100)

Sami Paavilainen[1,3] and Mats Persson[2,3]
[1]*Institute of Physics, Tampere University of Technology, 33720 Tampere, Finland*
[2]*Surface Science Research Centre and Department of Chemistry, The University of Liverpool, Liverpool, L69 3BX, United Kingdom*
[3]*Department of Applied Physics, Chalmers University of Technology, SE-412 96 Göteborg, Sweden*
(Received 24 April 2006; published 25 August 2006)

We have carried out a computational study of the inelastic electron tunnelling spectrum (IETS) of the two vibrational modes of a single hydrogen atom on a Cu(100) surface in a scanning tunnelling microscopy (STM) junction. This study addresses key issues about vibrational assignment and line shape of observed peaks in IETS within the framework of density functional theory calculations and the Lorente-Persson theory for STM-IETS. We argue that the observation of only a single broad peak in the STM-IETS [L. J. Lauhon and W. Ho Phys. Rev. Lett. **85**, 4566 (2000)] is not caused by any symmetry restrictions or any cancellation between inelastic and elastic vibrational contributions for one of the two modes but is due to strongly overlapping superposition of the contributions from the two modes caused by the rather large instrumental broadening and the narrow vibrational energy separation between the modes. In particular, we find that this broadening and the large asymmetry of the vibrational line shapes gives rise to substantial apparent vibrational energy shifts of the two modes and decreases their apparent energy separation.

DOI: 10.1103/PhysRevB.74.085417 PACS number(s): 73.20.Hb, 68.37.Ef, 68.43.Pq

## I. INTRODUCTION

A most important advance in surface science and nanoscience has been the realization of single-molecule vibrational spectroscopy and microscopy at metal surfaces using a scanning tunnelling microscope (STM).[1] The unique capabilities of the STM are based on two key ingredients: (i) the highly localized tunnelling of electrons in the space between the tip and the sample, resulting in atomic scale resolution in imaging, and (ii) the nonadiabatic coupling between tunnelling electrons and the vibrations in the STM junction giving rise to characteristic signatures in the tunnelling current $I$ at biases $V$ corresponding to vibrational energies. Usually, these thresholds are identified as peaks in the $\frac{d^2I}{dV^2}(V)$ signal. The observed vibrational energies provide information about the chemical identity of single adsorbed species and can also be used to discriminate among various isotopes. To fully exploit this vibrational spectroscopy, one needs physical insight from theory about the strengths, line shapes, and lateral spatial distributions of the vibrational signatures in the $\frac{d^2I}{dV^2}(V)$ signal.

The theory of inelastic electron tunnelling spectroscopy (IETS) from vibrations in a STM junction has been developed at various levels of sophistication by several groups.[2–5] One important advance was made by Lorente and Persson (LP),[4,6] who generalized the widely used Tersoff-Hamann theory for elastic tunnelling to inelastic tunnelling from vibrations and implemented the theory in density functional theory (DFT) calculations. As demonstrated by a direct comparison of the results from the LP theory with IETS experiments, this theory is able to reproduce the observed strengths of various vibrational modes for single molecules on a copper surface.[4,6–8] In particular, the LP theory suggested that many modes were not observed due to a cancellation between inelastic and elastic contributions to the tunnelling current. Furthermore, the results of the LP theory suggested a symmetry selection or rather propensity rule for IETS relating the symmetry of the vibrational mode, the spatial distribution of the inelastic signal and the tip orbital.[9] The existence of such a rule is of key importance in the assignment of various peaks in the IETS to vibrational modes.

A most simple system that raises issues about the role of symmetry and the assignment in IETS is provided by H and D atoms adsorbed on Cu(100). In these experiments by Lauhon and Ho,[10] IETS was used in a beautiful manner to discriminate between the H and D atoms, enabling the study of the isotope effect on surface diffusion. However, they observed only a single broad peak that was attributed to the perpendicular vibrational mode. This observation raises questions about the origin of the large broadening of the observed peak and why the parallel mode is not observed.

In this paper, we present a theoretical study of the IETS of H and D atoms on a Cu(100) surface based on the LP theory and DFT calculations. In particular, we clarify the origin of the observed single broad peak in the IETS in terms of strongly overlapping contributions from both the perpendicular and parallel vibrational modes, caused by the extrinsic broadening and the intrinsic asymmetry of the vibrational line shape. Before presenting and discussing our results, we begin with a short review of the necessary concepts and ingredients of the theory and the calculations of IETS.

## II. THEORY

The LP theory of STM-IETS is based on the simple and physically transparent Tersoff-Hamann (TH) theory for imaging by elastic electron tunneling.[11] TH theory is based on a simple tip model in which an emitted electron is approximated by an $s$ wave and the Bardeen approximation for tunnelling. Using these approximations, one obtains that the differential conductance, $\frac{dI}{dV}(V)$, at small biases, $V$, and low temperatures is simply determined by the local density of sample states (LDOS) at the position $\vec{r}_0$ of the tip apex as

 

$$\frac{dI}{dV}(V) \propto \rho(\vec{r}_0, \epsilon_F + eV), \tag{1}$$

where $\epsilon_F$ is the sample Fermi energy. In an one-electron approximation, as provided by density functional theory, $\rho(\vec{r}, \epsilon)$ is given by

$$\rho(\vec{r}, \epsilon) = \sum_\alpha |\langle \vec{r}_0 | \psi_\alpha \rangle|^2 \delta(\epsilon_\alpha - \epsilon), \tag{2}$$

where $\langle \vec{r}_0 | \psi_\alpha \rangle$ is an one-electron wave function with energy $\epsilon_\alpha$.

The LP theory is based on the observation that the TH theory for elastic tunnelling can be directly generalized to inelastic tunnelling from adsorbate vibrations by considering the many-body LDOS for the electrons interacting with the adsorbate vibrations. This result is based on a few physical assumptions that are fulfilled in most cases. First, the electron-vibration coupling is assumed to be short ranged and limited to the sample. Second, the vibrational relaxation rate should be much more rapid than the tunnelling rate, so that the vibration is nearly equilibrated. Third, the electron-vibration coupling is weak so that the vibration-induced LDOS $\Delta\rho$ can be evaluated by first-order perturbation theory. This nonadiabatic coupling gives rise to two distinct contributions to $\Delta\rho$—one from opening up an inelastic channel for tunnelling and one from its influence on the elastic tunnelling channel.

The channel for inelastic tunnelling from a vibration with vibrational frequency $\Omega$ opens up when the bias $V$ is larger than $\hbar\Omega/e$ and increases, in general, the tunnelling current. This threshold in $I$ results in a positive peak in the line shape function

$$L_0(V) \equiv \frac{d^2I}{dV^2}(V)/\rho_{bg}, \tag{3}$$

where $\rho_{bg}$ is the LDOS associated with the background differential conductance $(dI/dV)_{bg}$. The integrated strength $\eta_{inel}(\vec{r}_0)$ is given by the inelastic fraction of the tunnelling electrons with an energy larger than $\hbar\Omega$. In the quasistatic limit, $\Omega \to 0$, this fraction is given by the vibration-induced deformation of the vacuum tails of the one-electron wave functions as

$$\eta_{inel}(\vec{r}_0) = \sum_\alpha |\langle \vec{r}_0 | \delta\psi_\alpha \rangle|^2 \delta(\epsilon_\alpha - \epsilon_F)/\rho_{bg}. \tag{4}$$

Here, $\langle \vec{r}_0 | \delta\psi_\alpha \rangle$ is the change in $\langle \vec{r}_0 | \psi_\alpha \rangle$ by an rms displacement $\sqrt{\hbar/2m\Omega}$ of the vibrational mode.

The nonadiabatic coupling of the tunnelling electrons with the adsorbate vibration also affects the elastic tunnelling channel at the threshold for the inelastic tunnelling channel through the Pauli exclusion principle. This will show up as a decreased integrated strength and an asymmetry of the vibrational line shape, as given by

$$L_0(V) = \frac{\eta(\vec{r}_0)(\gamma/2) + \chi(\vec{r}_0)(eV - \hbar\Omega)}{\pi[(eV - \hbar\Omega)^2 + (\gamma/2)^2]}. \tag{5}$$

Here, the total integrated strength $\eta(\vec{r}_0) = \eta_{inel}(\vec{r}_0) + \eta_{el}(\vec{r}_0)$ has a negative contribution from the elastic channel given by

$$\eta_{el}(\vec{r}_0) = -\frac{2}{\rho_{bg}} \sum_\alpha |\mathrm{Im}(\langle \delta\psi_\alpha | \vec{r}_0 \rangle)|^2 \delta(\epsilon_\alpha - \epsilon_F). \tag{6}$$

The asymmetry parameter $\chi(\vec{r}_0)$ is given by,

$$\chi(\vec{r}_0) = -\frac{2}{\rho_{bg}} \sum_\alpha \mathrm{Re}(\langle \vec{r}_0 | \delta\psi_\alpha \rangle)\mathrm{Im}(\langle \delta\psi_\alpha | \vec{r}_0 \rangle) \delta(\epsilon_\alpha - \epsilon_F) \tag{7}$$

The remaining parameter determining the line shape in Eq. (5) is the vibrational relaxation rate $\gamma$.

For high-frequency adsorbate vibrations on metal surfaces, such as vibrations of H (and D) atoms on a Cu surface, $\gamma$ is dominated by the absorption and emission of single electron-hole pairs. The electron-hole pair contribution $\gamma_{eh}$ to $\gamma$ can be calculated also in the quasistatic limit from,[12]

$$\gamma_{eh} = 4\pi\Omega \sum_{\alpha,\beta} |\langle \psi_\alpha | \delta v | \psi_\beta \rangle|^2 \delta(\epsilon_\alpha - \epsilon_F) \delta(\epsilon_\beta - \epsilon_F). \tag{8}$$

Here $\delta v$ is change of the one-electron potential induced by an rms displacement of the vibrational coordinate.

The density functional theory calculations of the electronic and geometric structure of an H atom on a Cu(100) surface were carried out using Vienna *ab initio* simulation package VASP.[13] The electron ion core interactions were handled by the plane wave projector augmented wave (PAW) method[14] and exchange-correlation effects by a generalized gradient approximation.[15] Because of the large lateral extension of the STM image and IET signals, we have to use a large $6\times6$ supercell with Cu atoms in six layers, separated by a vacuum region corresponding to five layers of atoms. For this large supercell, it was sufficient to sample the Brillouin zone with a $2\times2\times1$ mesh. A cutoff energy of 20 Ry for the plane waves was found to be sufficient. In the calculations, the H/Cu(100) system was first geometrically optimized until forces on each ion were smaller than 0.02 eV/Å. The technical details about the calculations of the electron-vibration matrix elements and the vacuum tails of the wave functions, and the handling of the discrete set of electron states can be found in Ref. 6.

## III. RESULTS

The experimentally determined fourfold hollow adsorption site[10] was chosen as the initial configuration in the calculations. This site has been shown to be the energetically preferred site also in previous DFT studies.[16,17] After full structural relaxation, the vertical equilibrium distance of hydrogen from the uppermost copper layer was 0.58 Å. The nearest-neighboring copper atoms to the hydrogen atom relaxed 0.04 Å outward from the surface layer and $<0.02$ Å parallel to the surface away from the hydrogen adsorption site. Relaxations of the other copper atoms were found to be much smaller. The calculated adsorption energy −0.182 eV

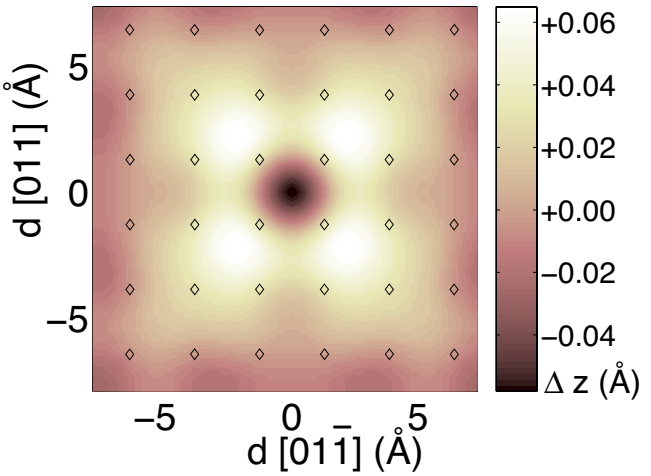


FIG. 1. (Color online) Topographical image of constant LDOS of an H atom adsorbed in the hollow site on a Cu(100) surface. $\Delta z$ is the change in tip-surface distance from its value of 6.26 Å away from the H atom. The positions of the Cu atoms in surface layer are indicated by the open diamonds.

relative to the binding energy of the H atom in the free $H_2$ molecule $\left(E_{\mathrm{ads}}=E_{\mathrm{H/Cu(100)}}-E_{\mathrm{Cu(100)}}-\frac{1}{2}E_{\mathrm{H_2}}\right)$ is in good agreement with the value −0.179 eV obtained by previous DFT calculations.[16]

In Fig. 1, we show the topographical image of constant LDOS of the H adatom at a typical value for the tip-surface distance. The main characteristic feature of this weakly corrugated image is the 0.05 Å depression at the adsorption site surrounded by four 0.06 Å protrusions centered close to the nearest-neighboring hollow sites in the [001] and [010] directions. The shape of the image with the single depression surrounded by the four protrusions is robust for all tip-surface distances between 5 and 10 Å. However, the depression at the hydrogen site decreases in depth with increasing tip-surface distance $z_0$: the depth decreases from 0.07 to 0.03 Å when $z_0$ increases from 5 to 8 Å. Note that the overall size of the affected area, about $10\times10$ Å$^2$, is very large compared to the size of hydrogen atom. All the features in the simulated STM image are in excellent agreement with the experimental image.[10]

The origin of the protrusions in the STM image is not simply due to the outward relaxation of the nearest-neighboring copper atoms or any H-induced state at the Fermi level. The protrusions still exist in the simulated image of the H atom on the unrelaxed, bare Cu surface. In accordance with the common picture of the H chemisorption,[18] the H atom induces an *s*-like state just below the onset of the Cu *d* band about 7 eV below the Fermi level. The small depression in the simulated image and the surrounding protrusions then originates from the orthogonalization of the metal states at the Fermi level against the H-induced state and also from the oscillatory screening response by the metal states of the $H^-$ entity.

The H adatom has two vibrational modes that, in principle, can contribute to the IET vibrational spectra. In the harmonic approximation, the calculated vibrational energies of the perpendicular mode and the twofold degenerate parallel mode are 84 and 68 meV, respectively.[19] These values are somewhat different from the corresponding values of 76 and 70 meV (Ref. 16) [71 and 62 meV (Ref. 17)] found in earlier density functional calculations, which take into account anharmonic effects. In these calculations, the vibrational excitation energies were determined from the energies of the ground state and the first excited states of $A_1$ and $E$ symmetry character in the full potential energy surface. These results are in better agreement with the experimental value of 70 meV (Ref. 20) for the dipole active (perpendicular) mode and will be used in the detailed comparison to the IET experiments.

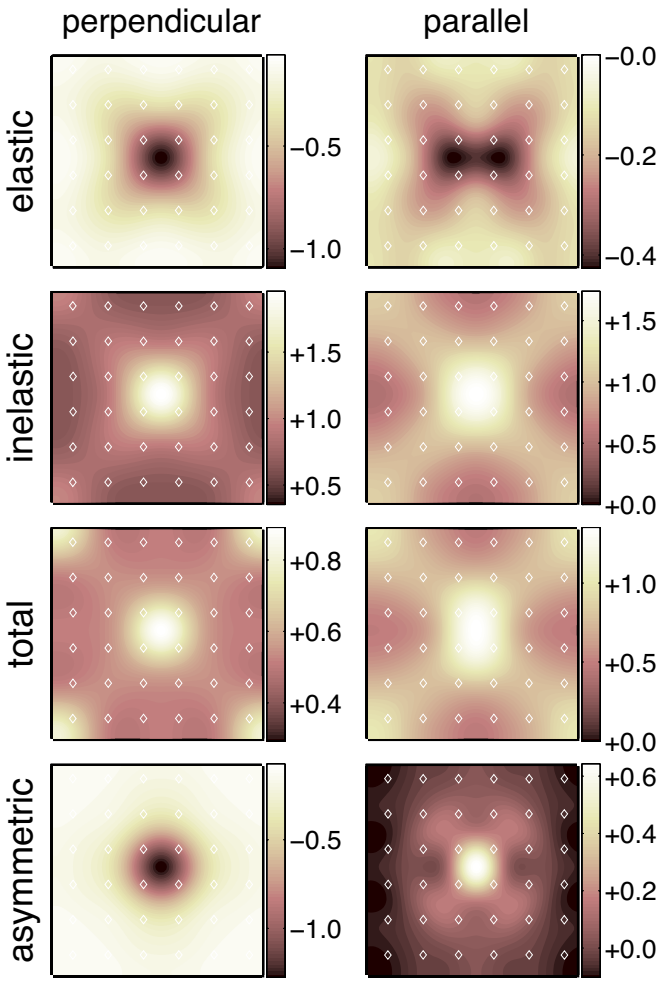


FIG. 2. (Color online) The first three rows of the columns show the spatial maps of the calculated elastic, inelastic, and total signal strengths for the perpendicular (left column) and the parallel mode vibrating in [01$\bar{1}$] direction (right column), respectively. The fourth row of figures show the spatial map of the calculated asymmetry parameter for each mode. The color scale in each subfigure stands for the percentual change in the current. The H atom is located at the center of the images, and the position of the Cu atoms in the surface layer are indicated by open diamonds. The $x$ and $y$ axes correspond to the [01$\bar{1}$] and [011] crystal directions, respectively. Each image has the same size of 15.4 Å$\times$15.4 Å. The tip-surface distance is 7 Å in all figures.

In Fig. 2, we depict the two-dimensional contour plots of the calculated IET line shape parameters $\eta_{\mathrm{el}}(\vec{r}_0)$, $\eta_{\mathrm{inel}}(\vec{r}_0)$,

$\eta_{\mathrm{tot}}(\vec{r}_0)$, and $\chi(\vec{r}_0)$, as defined in Eqs. (4), (6), and (7), around the H atom for the two vibrational modes.[21] For the doubly degenerate parallel modes, it is sufficient to map out the IET line shape parameters of the mode with a vibrational displacement in $[01\bar{1}]$ direction since for the other degenerate mode (with a displacement in the $[0\bar{1}1]$ direction) the parameters are simply obtained by rotating the maps 90 deg. The parallel mode parameters are then obtained simply as a sum of the contributions from the two degenerate modes.

The vibrational inelastic and elastic signals behave differently for the two vibrational modes. In the case of the perpendicular mode, both $\eta_{\mathrm{el}}(\vec{r}_0)$ and $\eta_{\mathrm{inel}}(\vec{r}_0)$ are peaked on top of the H adsorption site and cancel each other to a large extent. The extreme values for $\eta_{\mathrm{el}}(\vec{r}_0)$ and $\eta_{\mathrm{inel}}(\vec{r}_0)$ are $-1.1\%$ and 2.0%, respectively, so that $\eta_{\mathrm{tot}}(\vec{r}_0)$ has a maximum value of 0.9% on top of the H atom.[22] In contrast, there is no near cancellation of $\eta_{\mathrm{el}}(\vec{r}_0)$ and $\eta_{\mathrm{inel}}(\vec{r}_0)$ for the parallel mode. Thus, the extreme value of 1.4% for $\eta_{\mathrm{tot}}(\vec{r}_0)$ is stronger than for the perpendicular mode despite that the extreme values $-0.4\%$ and 1.4% for $\eta_{\mathrm{el}}(\vec{r}_0)$ and $\eta_{\mathrm{inel}}(\vec{r}_0)$, respectively, are both weaker than the corresponding values for the perpendicular mode.[22] Furthermore, the extreme value of $\eta_{\mathrm{tot}}(\vec{r}_0)$ from the twofold degenerate parallel modes will be twice as large since this value is attained at the symmetrical site on top of the H atom. Note that the IET line shape parameters depend somewhat on the tip-surface distance; maps in Fig. 2 correspond to a typical distance of 7 Å.[23]

Although the perpendicular and parallel vibrational modes have different symmetry characters ($A_1$ and $E$), the proposed symmetry selection rule in Ref. 9 or rather the symmetry propensity rule for IET does not give any definite predictions about the strengths and spatial behaviors of the inelastic and elastic signals for these two modes in this case. The effect of the H atom on the states around the Fermi level is minute, as demonstrated by the small corrugation of the calculated topographical image of the H atom. This result shows that the LDOS at the Fermi level and around the H atom will not be dominated by states with a definite symmetry character. Thus, there will be no significant symmetry restrictions for the IET in this case. As shown in Fig. 2, this fact is reflected by the spatial maps of $\eta_{\mathrm{tot}}$ being qualitatively same for the perpendicular and parallel vibrational modes. Hence, these maps cannot simply be used to discriminate between these two modes.

One qualitative difference in the IET from the two vibrational modes is the sign of the asymmetry parameter $\chi(\vec{r}_0)$, which has important implications for the vibrational line shapes in the IETS. At the H site, $\chi(\vec{r}_0)$ for the perpendicular mode is negative with an extreme value of $-1.2\%$, whereas for the parallel mode it is positive with an extreme value of 0.7%. Both these values are comparable in magnitude to $\eta_{\mathrm{tot}}(\vec{r}_0)$ and should give rise to vibrational IETS line shapes with characteristic asymmetries for the two modes. To show that, we need first to include the calculated vibrational line widths, obtained from Eq. (8), into Eq. (5) describing the vibrational line shapes. The electron-hole pair line widths $\gamma_{eh}$ are 1.8 and 1.1 meV for the parallel and perpendicular modes of the H adatom, respectively.[24] The corresponding relaxation rates $2.7\times10^{12}$ s$^{-1}$ and $1.6\times10^{12}$ s$^{-1}$ are much larger than the tunnelling rate $I/e\sim10^{9}$ s$^{-1}$ corresponding to the 0.1 nA current used in the experiments.[10] Thus, the current-induced nonequilibrium population of the mode should be small justifying one of the assumptions behind the LP theory that the vibration should be close to equilibrium.

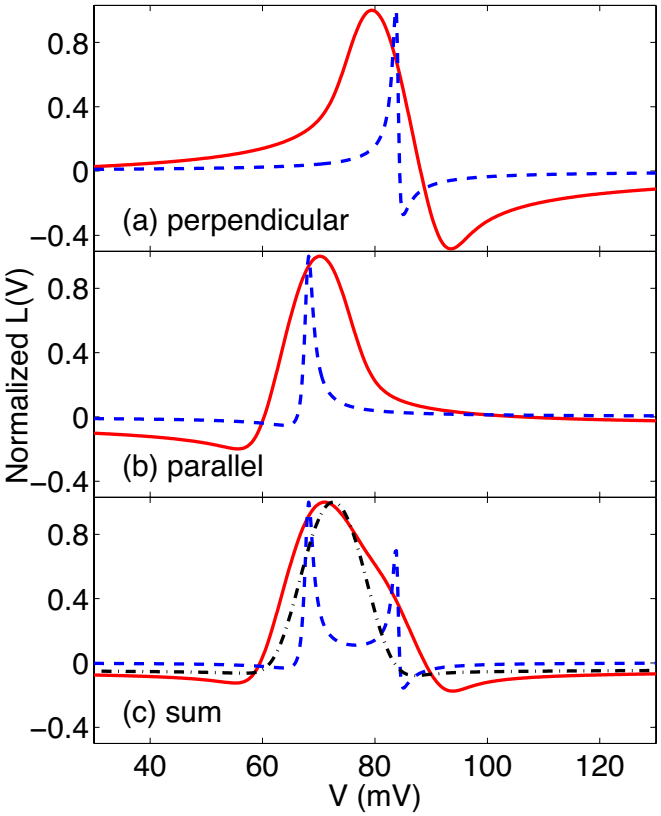


FIG. 3. (Color online) Calculated line shapes of the normalized second-order differential conductance for (a) the perpendicular mode, (b) the doubly degenerate parallel mode, and (c) the sum of the modes. The intrinsic line shapes are shown as dashed lines, whereas the line shapes that include temperature and modulation effects are shown as solid lines. All these line shapes are obtained using the calculated vibrational energies of 68 and 84 meV for perpendicular and parallel modes, respectively, as obtained in the harmonic approximation. The calculated line shape based on calculated vibrational energies (71 and 76 meV for the perpendicular and parallel, respectively) from Ref. 16, which takes into account anharmonicity and includes temperature and modulation effects, is shown as a dashed-dotted line in (c). The conductances correspond to a tip-surface distance of 7 Å with the tip on top of the H atom and $\eta$=1.4(0.9)%, $\chi$=0.7(−1.2)%, and $\gamma$=1.79(1.06) meV for the twofold degenerate parallel mode (perpendicular mode), respectively.

In Fig. 3, we show calculated vibrational IET line shapes for the two modes of the H adatom with the tip on top of the H atom. The intrinsic line shapes $L_0(V)$ (dashed lines) calculated from Eq. (5) are clearly narrow and asymmetric as shown in Figs. 3(a) and 3(b). Thus, we would expect that the IETS should have two clearly resolved peaks in apparent conflict with the single broad peak in the IETS observed by Lauhon and Ho.[10] However, the theory can be reconciled with experiments by taking into account the large extrinsic broadening provided by the temperature smearing of the tip

and sample Fermi distributions, and the modulation voltage.[25] In the experiments by Lauhon and Ho,[10] the modulation voltage had an rms value of 7 mV and the temperature was 9 K. Including these broadenings for the two modes results in the extrinsic line shape shown as solid lines in Figs. 3(a)–3(c). The large extrinsic broadening and the opposite asymmetries of the two line shapes result in broad peaks that are significantly red- and blueshifted for the perpendicular and parallel modes, respectively. In addition to decreasing the apparent energy separation between the peaks, the broadening is so large that the two peaks overlap strongly and can no longer be resolved as two peaks. This effect is even more pronounced when using the more precise values of 71 and 76 meV for the vibrational excitations obtained from Ref. 16. Finally, the calculated total strength of the IET from the two modes is about 2–3%, depending on the distance, which is in reasonable agreement with estimate of $\sim 1.1\%$ for the observed peak in the IETS. The theoretical isotope dependence $m^{-1}$ of $\eta_{\mathrm{tot}}$ with the atomic mass $m$ is consistent with the observed isotope dependence of the intensity for the H and the D atoms.

## IV. SUMMARY

We have carried out a computational study of the inelastic electron tunnelling spectrum (IETS) of the two vibrational modes of a single hydrogen atom on a Cu(100) surface in a scanning tunnelling microscopy (STM) junction. This study addresses key issues about vibrational assignment and line shape of observed peaks in IETS and is based on density functional theory calculations and the Lorente-Persson theory for STM-IETS. We argue that the observation of only a single broad peak is not caused by any symmetry restrictions or any cancellation between inelastic and elastic vibrational contributions for one of the two modes but is rather a superposition of the contributions from the two modes caused by the large instrumental broadening and their narrow vibrational energy separation. In particular, we find that this broadening and the large asymmetry of the vibrational line shapes gives rise to substantial apparent vibrational energy shifts between the two modes and decreases their apparent energy separation.

## ACKNOWLEDGMENTS

We acknowledge partial funding by the EU-RTN project "AMMIST," the Swedish Research Council (VR), and the Academy of Finland. Allocation of computer resources by SNAC is also gratefully acknowledged.

[1] B. C. Stipe, M. A. Rezaei, and W. Ho, Science **280**, 1732 (1998).
[2] B. N. J. Persson and A. Baratoff, Phys. Rev. Lett. **59**, 339 (1987).
[3] N. Mingo and K. Makoshi, Phys. Rev. Lett. **84**, 3694 (2000).
[4] N. Lorente and M. Persson, Phys. Rev. Lett. **85**, 2997 (2000).
[5] T. Mii, S. Tikhodeev, and H. Ueba, Surf. Sci. **502/503**, 26 (2002).
[6] N. Lorente and M. Persson, Faraday Discuss. **117**, 277 (2000).
[7] M. Persson, Philos. Trans. R. Soc. London, Ser. A **362**, 1173 (2004).
[8] M.-L. Bocquet, H. Lesnard, and N. Lorente, Phys. Rev. Lett. **96**, 096101 (2006).
[9] N. Lorente, M. Persson, L. J. Lauhon, and W. Ho, Phys. Rev. Lett. **86**, 2593 (2001).
[10] L. J. Lauhon and W. Ho, Phys. Rev. Lett. **85**, 4566 (2000).
[11] J. Tersoff and D. R. Hamann, Phys. Rev. Lett. **50**, 1998 (1983).
[12] B. Hellsing and M. Persson, Phys. Scr. **29**, 360 (1984).
[13] G. Kresse and J. Furthmüller, Phys. Rev. B **54**, 11169 (1996).
[14] G. Kresse and D. Joubert, Phys. Rev. B **59**, 1758 (1999).
[15] J. P. Perdew, J. A. Chevary, S. H. Vosko, K. A. Jackson, M. R. Pederson, D. J. Singh, and C. Fiolhais, Phys. Rev. B **46**, 6671 (1992); Y. Wang and J. P. Perdew, *ibid.* **44**, 13298 (1991).
[16] P. G. Sundell and G. Wahnström, Phys. Rev. B **70**, 081403(R) (2004).
[17] W. Lai, D. Xie, J. Yang, and D. H. Zhang, J. Chem. Phys. **121**, 7434 (2004).
[18] H. Hjelmberg, Phys. Scr. **18**, 481 (1978).
[19] The vibrational energies were calculated by slightly displacing the H atom from its adsorption site and using the harmonic approximation for the perturbed energies.
[20] I. Chorkendorff and P. B. Rasmussen, Surf. Sci. **248**, 35 (1991).
[21] The calculations were carried out with the same displacements of the hydrogen atom as for the calculation of the vibrational energies.
[22] The maximum values depend on the parameter $\sigma$ used to broaden the discrete states. For parallel mode using $\sigma=0.2$ eV gives a maximum $\eta_{\mathrm{tot}}(\vec{r}_0)$ of 1.2% and $\sigma=0.3$ eV 0.7%. For perpendicular mode with $\sigma=0.2$ and 0.3 eV, the maximum of $\eta_{\mathrm{tot}}(\vec{r}_0)$ are 1.9% and 1.1%, respectively. The spatial distribution of the signal is however not sensitive to the choice of $\sigma$. All the results shown correspond to $\sigma=0.25$ eV unless mentioned otherwise.
[23] The total relative change across the perpendicular mode diminishes from 1.7% to 0.9% when increasing tip-surface distance from 5 to 10 Å. For the same distance range, the elastic signal increases from −0.6% to −0.3%, inelastic signal is weakened from 2.3% to 1.2%, and asymmetry parameter from 1.1% to 0.8%. For parallel mode, the changes are smaller; total relative changes goes from 1.1% to 0.9%, elastic signal from 1.2% to 0.9%, inelastic from 2.4% to 1.7%, and asymmetry parameter from −1.5% to −1.1% for the corresponding distance range.
[24] These values are not very sensitive to the used broadening of the states. For $\sigma=0.20$ (0.30) eV, the values were 1.85 (1.74) meV, and 0.94 (1.12) meV for the perpendicular and parallel mode, respectively.
[25] The broadenings caused by the modulation voltage with amplitude $\delta V$ and the tip and sample temperature $T$ were obtained by multiplying $L_0(V)$ in the Fourier time ($\tau$) domain by $2J_2(\delta V\tau)/\tau^2$ and $(\pi k_B T\tau)^2/\sinh^2(\pi k_B T\tau)$.